Effects of size polydispersity on the extinction spectra of colloidal nanoparticle aggregates

Alexander E. Ershov,[1,2] Ivan L. Isaev,[1] Polina N. Semina,[1] Vadim A. Markel,[3] and Sergei V. Karpov[1,2]
[1]*L. V. Kirenskiy Institute of Physics, Russian Academy of Sciences, Kransoyarsk, 660036, Russian Federation*
[2]*Siberian Federal University, Krasnoyarsk, 660041, Russian Federation*
[3]*Department of Radiology, Department of Bioengineering, and the Graduate Group in Applied Mathematics and Computational Science, University of Pennsylvania, Philadelphia, Pennsylvania 19104, USA*
(Received 2 June 2011; revised manuscript received 23 December 2011; published 12 January 2012)

We investigate the effect of particle polydispersity on the optical extinction spectra of colloidal aggregates of spherical metallic (silver) nanoparticles, taking into account the realistic interparticle gaps caused by layers of stabilizing polymer adsorbed on the metal surface (adlayers). The spectra of computer-generated aggregates are computed using two different methods. The coupled-multipole method is used in the quasistatic approximation and the coupled-dipole method beyond the quasistatics. The latter approach is applicable if the interparticle gaps are sufficiently wide relative to the particle radii. Simulations are performed for two different particle size distribution functions (bimodal and Gaussian), varying the number of particles per aggregate, and different distribution functions of the interparticle gap width. The strong influence of the latter factor on the spectra is demonstrated and investigated in detail.

DOI: 10.1103/PhysRevB.85.045421 PACS number(s): 78.67.Bf, 41.20.Cv, 73.20.Mf

I. INTRODUCTION

The optical properties of noble-metal hydrosols containing nanoparticle aggregates with random, typically, fractal geometry have been in the focus of vigorous research since the mid-1980s.[1–7] Branched disordered aggregates of spherical nanoparticles with the average particle size of about 10 nm form in such hydrosols under the condition of low coagulation stability. The optical properties of these aggregates have attracted significant attention. The electromagnetic interaction of individual nanoparticles in an aggregate leads to a number of effects, some of which are of practical importance. In this regard, it is appropriate to mention the effect of optical memory[8–11] (spectrally selective photomodification) and the giant enhancement of optical nonlinearities.[12–18] In general, the physics of metal hydrosols is very rich. For example, a quantitative description of the optical memory effect requires the application of the methods of chemical kinetics, thermodynamics, and the theory of elasticity.[19,20]

Experimental studies of the extinction spectra of metal hydrosols allow one to test the applicability of various theoretical and numerical approaches to realistic systems. In particular, it can be expected that any such approach should, at least, reproduce the shape and extent of the experimentally observed long-wavelength tail in the extinction spectra of the hydrosols. Note that all physical effects of practical importance, including those mentioned above, occur at frequencies which are redshifted relative to the Fröhlich resonance of an isolated particle. It can be expected that the long-wavelength spectral tail is strongly affected by the degree of polydispersity of individual nanoparticles. Preparation of monodisperse colloids is experimentally problematic, and the commonly used colloids are polydisperse. However, the effects of polydispersity on the optical spectra of aggregates are not fully understood. In particular, the role of interparticle polymer layers (adlayers), which can also be polydisperse (that is, of varying width), has not been studied. The numerical simulations presented below are aimed at rectifying this situation.

Previous studies of the effects of polydispersity on the optical spectra of aggregates of spherical nanoparticles are few. Khlebtsov and Melnikov have studied the scattering structure factor $S_0(\mathbf{q})$ of polydisperse fractal aggregates,[21] where $\mathbf{q} = \mathbf{k} - \mathbf{k}'$ and the latter two quantities are the wave vectors of the incident and the scattered waves. The structure factor determines the differential scattering cross section of an object within the first Born approximation. It was found that polydispersity has almost no effect on S_0, except for a slight dependence observed when $|\mathbf{q}|R_g \sim 1$, R_g being the gyration radius of the aggregate. However, the first Born approximation cannot be used to describe plasmonic resonances, which occur due to strong multiple scattering. Perminov *et al.* have studied the problem numerically using the dipole approximation (DA) for two neighboring spheres[22] and for more complicated multiparticle aggregates.[23] In these references, multiple scattering and plasmonic resonances were included into consideration. The positions and oscillator strengths of these resonances are very sensitive to the separation and radii of neighboring nanoparticles. Correspondingly, it was found that polydispersity has a pronounced influence on the spectra, with the strongest electromagnetic interaction and the largest spectral shifts obtained when the neighboring particles are of the same size. More recently, Naeimi and Miri have studied[24] the extinction spectra of large polydisperse fractal aggregates with the number of particles up to $N = 10^3$. In this reference, the DA was also used but the consideration was restricted to the quasistatic regime. It was found that polydispersity has a strong effect on the spectra of fractal aggregates, with the maximum spectral shifts occurring in the monodisperse case. This finding is in agreement with Refs. 22 and 23.

While the studies mentioned above do shed light on the problem considered here, they do not include the effects of adlayers. In other words, it is assumed that the neighboring spherical particles touch to form self-supporting aggregates. In reality, this is not so. Indeed, to prevent rapid coagulation, a soluble polymer is commonly added into the colloidal solution. Each nanoparticle adsorbs the polymer or other molecules and is coated by an adsorption layer (adlayer). The minimum

thickness of the adlayer is ∼0.15 nm, which corresponds to the characterisic size of the low-molecular-weight fragments of the polymer chains. A larger adlayer width is obtained when larger fragments, containing multiple loops and branches, are tightly packed around the metal surface.[25] If elastic deformation of the adlayers is neglected, the interparticle gap width is equal to the sum of adlayers of the neighboring particles and can vary, in practice, from 0.2 to 2 nm. When elastic deformations are taken into account, the interparticle gaps can be somewhat smaller. The presence of adlayers can significantly modify the spectra. In particular, we will see below that, in certain cases, the polydispersity of particles (with adlayers taken into account) can *increase* the relative weight or the extent of the redshifted spectral resonances, contrary to the previous findings.[22–24]

Another reason that a closer look at the problem may be desirable is the use of the DA in the previous studies.[22–24] It is well known that the DA does not reproduce the experimentally observed long-wavelength tail of the extinction spectra, at least not without the introduction of phenomenological geometrical rescaling.[26] The inaccuracy of the DA for closely spaced particles has been well documented.[27] In some cases, e.g., when the number of particles in a cluster is large, the use of the DA is almost unavoidable. In particular, the DA can be easily formulated and used beyond the quasistatic regime. Correspondingly, we use the DA for larger clusters, which are not necessarily small compared to the incident wavelength. As was mentioned above, the DA is inaccurate for closely spaced particles. However, this problem is somewhat rectified by the presence of adlayers, which do not allow the metal cores to touch.

We have found numerically that, for the geometries considered in this paper, the inaccuracy of the DA becomes insignificant for interparticle gaps 5 nm and larger for particle radii $\lesssim 10$ nm. For particle radii $\lesssim$ (4–5) nm, gaps can be $\gtrsim$2 nm. For smaller interparticle gaps the inaccuracy of the DA can be minimized in the spectral range 350–600 nm with the introduction of a phenomenological rescaling parameter. The DA is used in this work both with and without the phenomenological rescaling[26] to compare the results.

In the case of smaller aggregates, we use a more rigorous approach, which is based on the coupled-multipole method. This method allows one to take into account the excitation of multipole moments of arbitrarily high order, subject only to computational constraints. In our implementation, the method is limited to quasistatics and used for aggregates containing up to $N = 50$ nanoparticles, taking into account the maximum multipole order $L = 40$ ($L = 65$ is used for verification of convergence in some cases).

II. THEORETICAL MODEL

Consider a plane electromagnetic wave of the form

$$\mathbf{E}_{\rm inc}(\mathbf{r},t) = \mathbf{E}_0 \exp[i(\mathbf{k}\cdot\mathbf{r} - \omega t)] \tag{1}$$

incident on an aggregate of N spherical nanoparticles. The radii and radius vectors of the sphere centers are denoted by a_n and $\mathbf{r}_n, n = 1,2,\ldots,N$. The condition of nonintersection reads $|\mathbf{r}_n - \mathbf{r}_m| \geqslant a_n + a_m$ for all pairs (n,m). In the simulations presented below, the geometry of the aggregates is such that the strict inequality always holds due to the presence of adlayers. However, when geometrical rescaling[26] is used (within the DA), the radii and the interparticle distances are renormalized so that a geometrical intersection is possible.

We assume that the nanoparticles are made of silver whose permittivity ϵ has been tabulated in Ref. 28 for bulk samples at optical and near-IR frequencies. We use these data and take into account a finite-size correction to the Drude relaxation constant γ, as is explained below in Sec. II A. The host medium is assumed to be water and its permittivity is taken to be $\epsilon_h = 1.78$, independently of frequency. We take the permittivity of the polymer adlayers to be equal to ϵ_h. This is, of course, an approximation. The polymer may have a permittivity that is noticeably different from that of water. It is not even clear whether the approach based on the macroscopic Maxwell's equations is applicable to very thin adlayers. However, the approximations involved may be viewed as not too severe because, at optical and near-IR frequencies, both the polymer and the host medium are good dielectrics while the permittivity of metal cores is negative and very large in absolute value.

We use a truncated Gaussian and a bimodal distribution function for the particle radii. The former is obtained by truncating the Gaussian function

$$W(a) = \frac{1}{\sqrt{2\pi\sigma^2}} \exp\left(-\frac{(a - \langle a\rangle)^2}{2\sigma^2}\right) \tag{2}$$

by setting it to zero outside of a given interval $[a_1,a_2]$, where $0 < a_1 < a_2$, and renormalizing the resultant function to unity. We use $\langle a\rangle = \sigma = 10$ nm. In the case of the bimodal distribution, the particle radii can take only two discrete values a_1 and a_2, and each aggregate consists of equal numbers of particles of each kind. The average particle radius is in this case $\langle a\rangle = (a_1 + a_2)/2$, and we still require that $\langle a\rangle = 10$ nm. The geometry of typical aggregates obtained using the two different size distributions is illustrated in Fig. 1.

A. Account of finite-size effects

If the particle radii are small compared to the electron free path ℓ ($\ell \sim 50$ nm in silver), it is important to take into account the quantum finite-size effects on the permittivity of metal cores.[1,29,30] In the existing theoretical models, the most significant finite-size effect is the dependence of the Drude relaxation constant on the particle radius, which can be described by the formula

$$\gamma(a) = \gamma_\infty + \frac{v_F}{a}. \tag{3}$$

Here γ_∞ is the relaxation constant in bulk, v_F is the Fermi velocity of conduction electrons, and a is the nanoparticle radius. The modified relaxation constant can be substituted directly into the Drude formula. If tabulated data for the permittivity are used, as is the case here, we can follow the approach proposed in Ref. 31. That is, we subtract the Drude contribution from the bulk value of the permittivity and then add back a similar term but with a modified relaxation constant $\gamma(a)$, viz.,

$$\epsilon(a) = \epsilon_\infty + \frac{\omega_p^2}{\omega(\omega + i\gamma_\infty)} - \frac{\omega_p^2}{\omega[\omega + i\gamma(a)]}, \tag{4}$$

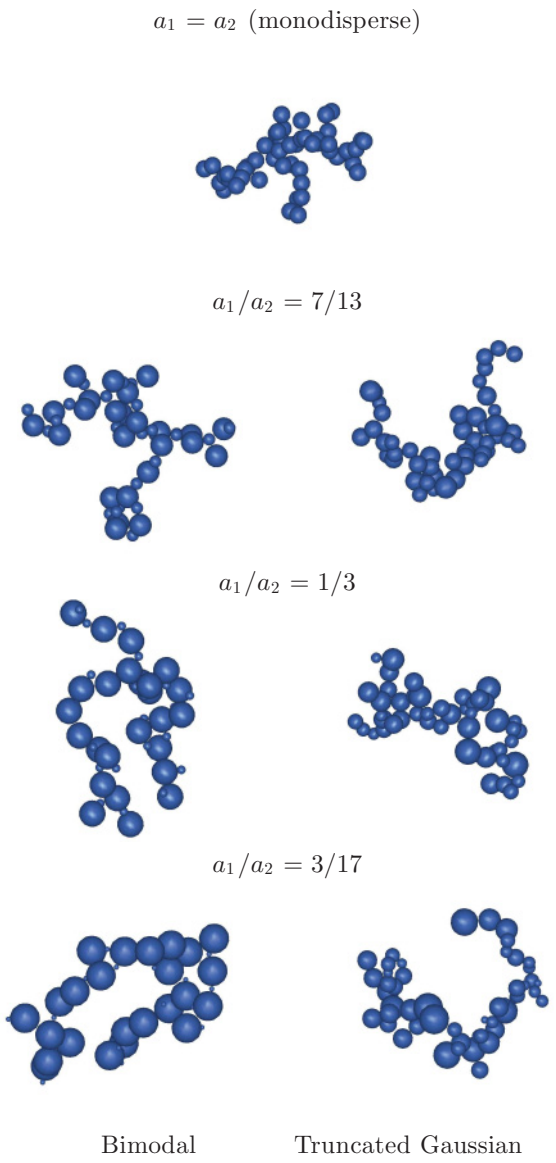

FIG. 1. (Color online) Illustration of the typical geometries of aggregates obtained using the two different size distributions.

where ϵ_∞ is the bulk value and ω_p is the plasma frequency. In the simulations, we take $\lambda_p = 2\pi c/\omega_p = 136$ nm, $\gamma_\infty/\omega_p = 0.002$, and $v_F/\gamma_\infty = 51$ nm. These numerical values of parameters are good approximations for silver.

It follows from (4) that the "effective" permittivity of the metal cores depends on the particle radius. Within the DA, this fact can be easily accounted for. However, the coupled-multipole method is ill suited for the case of compositional disorder. To bypass this difficulty, we adopt below an additional approximation (used only within the coupled-multipole method) in which the finite-size correction is computed for the average particle radius $\langle a \rangle = 10$ nm.

B. Coupled-multipole method for polydisperse aggregates

The quasistatic coupled-multipole method for polydisperse aggregates was formulated previously.[32] In Ref. 33, the method was derived for monondisperse aggregates in a form convenient for the continued fraction expansion, which is used in numerical simulations of this paper. We will, therefore, briefly describe a generalization of the formulas of Ref. 33 to the case of polydispersity. In this section, we refer to the equations of Ref. 33 using the notation (PRB-#), where # is the number of the equation, and use the indices n,n' instead of i,i' to label the particles.

(1) The quasistatic spherical harmonics defined in Eqs. (PRB-27) through (PRB-30) now take the form

$$\psi^{(1)}_{nlm}(\mathbf{r}) = \begin{cases} \left(\frac{r}{a_n}\right)^l Y_{lm}(\hat{\mathbf{r}}) & \text{if} \quad r \leqslant a_n, \\ 0 & \text{otherwise;} \end{cases} \tag{5a}$$

$$\mathbf{X}^{(1)}_{nlm} = \frac{1}{\sqrt{l a_n}} \nabla \psi^{(1)}_{nlm}(\mathbf{r} - \mathbf{r}_n);$$

$$\psi^{(2)}_{nlm}(\mathbf{r}) = \begin{cases} \left(\frac{a_n}{r}\right)^{l+1} Y_{lm}(\hat{\mathbf{r}}) & \text{if } r \geqslant a_n, \\ 0 & \text{otherwise;} \end{cases} \tag{5b}$$

$$\mathbf{X}^{(2)}_{nlm} = \frac{1}{\sqrt{(l+1) a_n}} \nabla \psi^{(2)}_{nlm}(\mathbf{r} - \mathbf{r}_n).$$

The functions defined above still satisfy the orthogonality properties (PRB-31)–(PRB-35), where a must be replaced by a_n.

(2) To calculate the overlap integral appearing in (PRB-37), the following changes must be made. In the definition of integration limits, a must be replaced by a_n in the first integral and by $a_{n'}$ in the second integral. In (PRB-38), a is replaced by a_n. Equations (PRB-39) through (PRB-43) remain unchanged while, in (PRB-44), the factor

$$\left(\frac{a}{r_{nn'}}\right)^{l+l'+1}$$

must be replaced by

$$\frac{a_n^{l+1/2} a_{n'}^{l'+1/2}}{r_{nn'}^{l+l'+1}}.$$

This replacement is the most significant mathematical difference between the cases of mono- and polydisperse aggregates. Indeed, the above factor enters the definition of the interaction matrix [see Eqs. (PRB-36) and (PRB-44)], which is directly used in all calculations. In particular, the extinction cross section can be computed by using (PRB-9) or (PRB-10). In this work, we use the method of expansion of the Green's function into a continued fraction, according to formulas (PRB0-48) and (PRB-49).

(3) Finally, in the expression (PRB-46) for $|E_0\rangle$, a should be replaced by a_n and the square root should be brought under the sign of summation.

C. Coupled-dipole method for polydisperse aggregates

The method described in Sec. II B is limited to the quasistatic approximation but allows one to consider interaction of particles with very small interparticle gaps. Generalization of this method beyond quasistatics is possible but computationally problematic. The coupled-dipole equations of the DA are well known and not repeated here. In a somewhat different physical context, these equations and the relevant mathematics can be found in Refs. 34 and 35 and, in application to the

problem at hand, in Refs. 31 and 36. The only two points to be made are the following. First, the polarizability of the n particle must be computed taking into account the polydispersity and the finite-size correction according to

$$\alpha_n = a_n^3 \frac{\epsilon(a_n) - \epsilon_h}{\epsilon(a_n) + 2\epsilon_h - i(2/3)(ka_n)^3[\epsilon(a_n) - \epsilon_h]}, \quad (6)$$

where $\epsilon(a_n)$ is the permittivity of the particle material computed according to (4) and $k = \omega/c$ is the vacuum wave number. We thus see that α_n depends on the particle radius not only because of the overall factor a_n^3 but also due to the radiative correction [the term proportional to $(ka_n)^3$] and to the finite-size effect. On the other hand, we have found that the higher multipole moments can be neglected if the interparticle gaps are $\gtrsim$5 nm for particle radii $\lesssim$10 nm. Second, to improve the accuracy of the DA, the renormalization parameter ξ has been previously introduced for the case of monodisperse particles.[26] Here we generalize this approach to the particle polydispersity. Namely, we define the rescaling parameter as $\xi = (a_n + a_{n'} + h)/r_{nn'}$, where h is the interparticle gap and $r_{nn'}$ is the distance between the centers of particles n and n'. When $\xi \geqslant 1$, $r_{nn'}$ decreases. The values of other parameters in the formula and the coordinates of particles in the aggregate remain unchanged ($\xi = 1$ corresponds to no rescaling). The magnitude of this parameter is defined empirically by comparing the simulated long-wavelength wing of the extinction band to the experimental spectra recorded for, approximately, the same geometry of aggregates. In this case, the DA can be used, and extension of this approach beyond quasistatics does not result in any difficulties.

D. Aggregation models

In this work, we employ the dynamical model of nanoparticle aggregation.[37] This model allows one to simulate the geometry of realistic, off-lattice polydisperse aggregates with various widths of the interparticle gaps. The model of Ref. 37 accounts for the van der Waals and elastic interactions of particles. We use three different modifications of this model, which differ in the initial distribution of the adlayer width and in the magnitude of the elasticity modulus of the adlayers. In particular, in the first two models the elasticity modulus is taken to be infinite and the elastic deformation of adlayers is ignored.

Aggregates of type 1. In the first modification, the initial adlayer thickness on each particle is proportional to its radius and the elasticity modulus of the adlayers is infinite. Consequently, there are no elastic deformations of the adlayers in the area of mechanical contact. In this case, the width of each interparticle gap is equal to the sum of initial adlayers of the neighboring particles.

Aggregates of type 2. Aggregates of type 2 are similar to those of type 1, but the initial width of all adlayers is constant and independent of the particle radii.

Aggregates of type 3. To generate aggregates with more realistic interparticle gaps, the Brownian dynamics method is used[37] with a self-consistent account of van der Waals and elastic forces. Unlike in aggregates of types 1 and 2, a realistic elasticity modulus of the adlayers is used. We start the simulations with the initial thicknesses of all adlayers being equal, as in the case of type-2 aggregates. However, the equilibrium values of the interparticle gaps are, generally, different from those in aggregates of type 2 because of elastic deformation of the adlayers. In particular, the equilibrium gaps between larger particles are reduced due to the stronger van der Waals attraction. Thus, the gaps are $\approx$0.3 nm for two neighboring particles with $a = 3$ nm, $\approx$0.2 nm for $a = 10$ nm, and $\lesssim$0.1 nm for $a = 17$ nm. Full details of the simulation are given in Ref. 37.

Note that aggregates of type 2 are obtained as special cases of aggregates of type 3 by setting the elasticity modulus to infinity.

III. RESULTS AND DISCUSSION

In this section, we report simulation results for the dimensionless extinction efficiency Q_e, defined as the ratio of the extinction cross section σ_e and the total geometrical cross sections of all particles in the aggregate, viz.,

$$Q_e = \frac{\langle \sigma_e \rangle}{\sum_{n=1}^{N} \pi a_n^2}, \quad (7)$$

where $\langle \sigma \rangle$ is the extinction cross section of an aggregate averaged over polarizations and propagation directions of the incident wave (1), with the exception of the spectra of dimers and trimers (Sec. III B), which are not averaged but rather computed for the incident polarization parallel and the incident wave vector perpendicular to the axis of symmetry of the system. The quantity Q is shown in all plots below.

A. Convergence of the coupled-multipole method

In order to verify the convergence of the numerical results with the maximum multipole order L, we computed the spectra of two identical nanoparticles with $a = 10$ nm and different values of the interparticle gap h (measured between the nearest points of the two spheres). We found that the spectrum has converged when $L \sim 40$ for $h = 0.2$ nm. However, larger values of L are required for $h \leqslant 0.1$ nm.

Previous studies have indicated[33] that the convergence condition on L is, approximately, the same for a multiparticle aggregate and for two neighboring particles (in the latter case, when the polarization of the external field is parallel to the axis of symmetry). Since further increase of L is impractical, we use $h \geqslant 0.2$ nm and $L = 40$ in the simulations reported below. This set of parameters is not too restrictive, guarantees convergence, and results in a reasonable computational time.

B. Spectra of polydisperse dimers and trimers

In Fig. 2, we plot the extinction spectra of a dimer—that is, of two spherical particles of radii a_1 and a_2 separated by the interparticle gap h. The incident polarization is parallel to the axis of symmetry of the dimer. As could be expected, for fixed radii of the spheres, the spectral shift and the amplitude of the long-wavelength spectral peak increase when h is decreased. For a fixed h, the spectral shift of this peak (but not the amplitude) decreases when the degree of polydispersity is increased. This is in a qualitative agreement with Refs. 22 and 23, which utilized the DA. However, unlike in Refs. 22 and 23, we have found that the amplitude of the long-wavelength

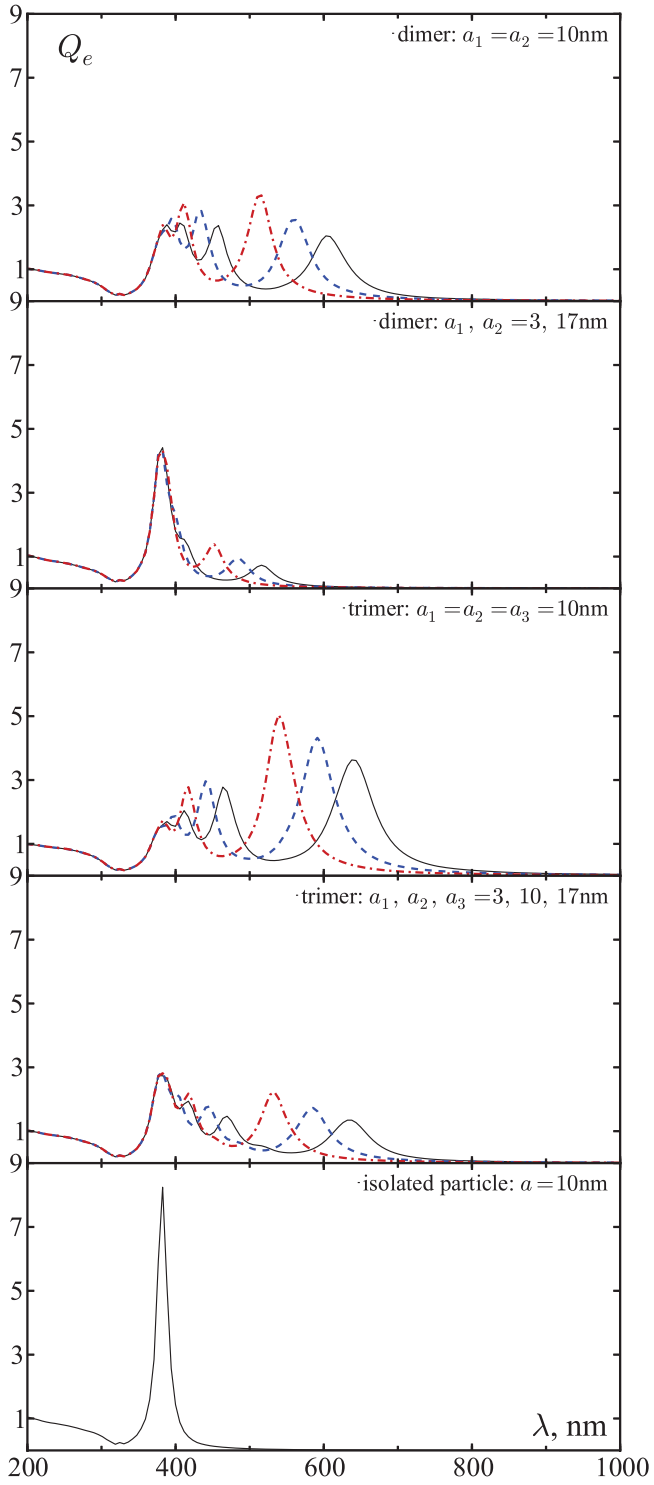

FIG. 2. (Color online) Extinction spectra of dimers, trimers, and an isolated spherical particle. The sphere radii and interparticle gaps are as labeled. The interparticle gap is $h = 0.2$ nm (solid black line); 0.3 nm (blue dashed line); 0.5 nm (red dot-dashed line).

peak noticeably increases when the degree of polydispersity is increased. This result is somewhat counterintuitive and cannot be obtained within the DA.

We now turn to a trimer consisting of three different-sized nanoparticles whose centers lie on the same line. Here the outlying spheres have the radii a_1 and a_2, which are varyable,

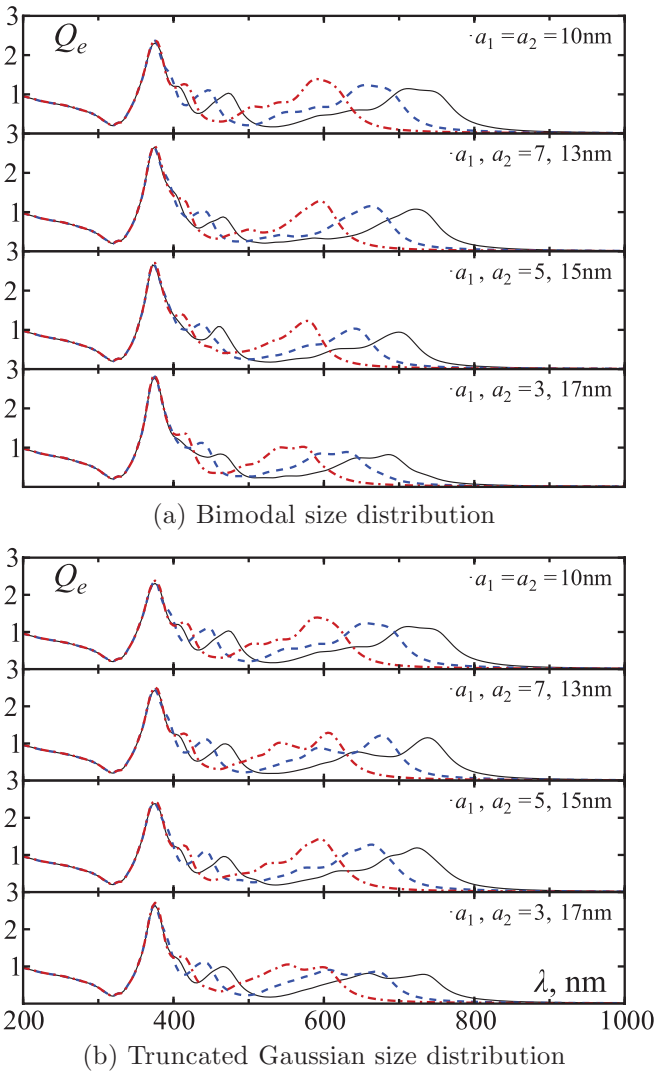

(a) Bimodal size distribution

(b) Truncated Gaussian size distribution

FIG. 3. (Color online) Extinction spectra of polydisperse aggregates of type 1 containing $N = 50$ nanoparticles computed by the coupled-multipole method for various size distribution functions, as labeled. Different curves correspond to different average values of the interparticle gap: $\langle h \rangle = 0.2$ nm (solid black line); 0.3 nm (blue dashed line); 0.5 nm (red dot-dashed line).

and the sphere in the center has the fixed radius 10 nm. The interparticle gaps are both equal to h. The external electric field is polarized parallel to the axis of symmetry. The extinction spectra for this system are shown in Fig. 2. The same qualitative conclusions can be made as in the case of the dimer. We note, however, that the long-wavelength peak for the trimer is shifted further toward the infrared.

C. Spectra of polydisperse multiparticle aggregates

1. Aggregates of type 1

The extinction spectra computed in the coupled-multipole method for this type of aggregate are shown in Fig. 3. It can be seen that, in the case of the bimodal distribution, the effect of polydispersity is to reduce the extent of the long-wavelength spectral tail, in qualitative agreement with the results of Refs. 22 and 23. In the case of the truncated

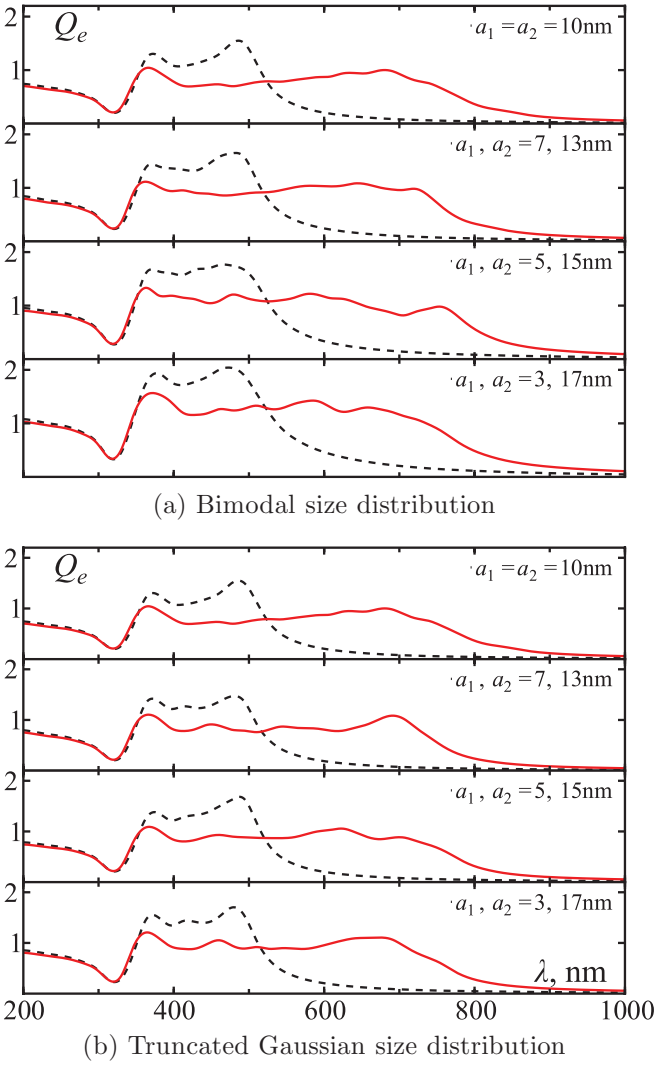

(a) Bimodal size distribution

(b) Truncated Gaussian size distribution

FIG. 4. (Color online) As in Fig. 3 but computed within the DA. Also, $\langle h \rangle = 0.2$ nm in all cases. Different curves correspond to different values of the rescaling parameter ξ (see Ref. 26). The black dashed line corresponds to $\xi = 1$ (no rescaling) and the red solid line corresponds to $\xi = 1.4$.

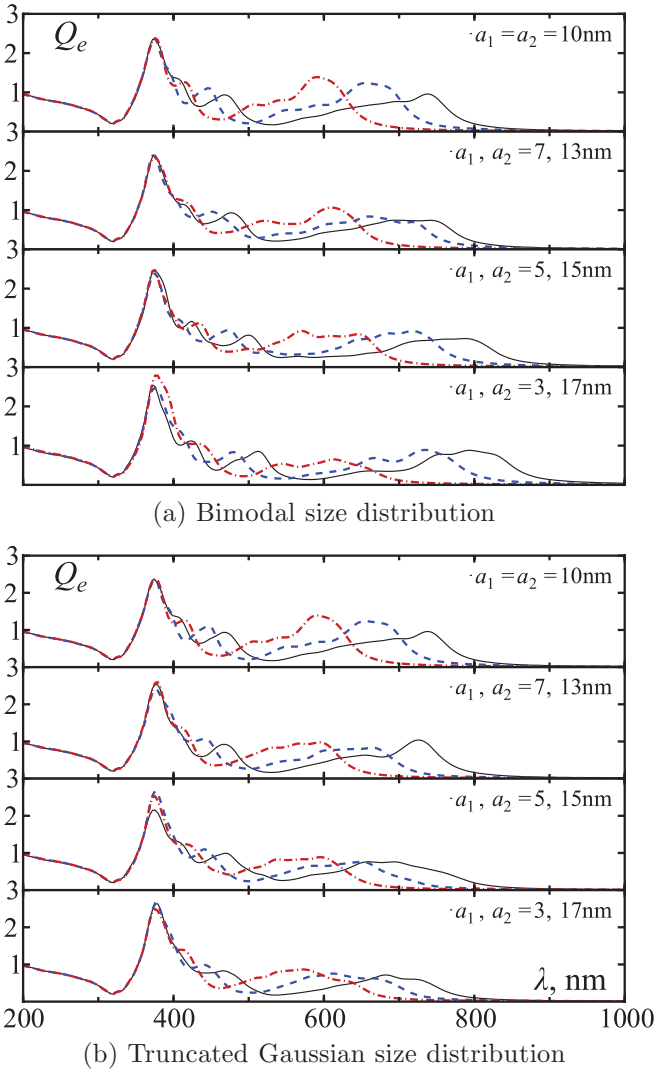

(a) Bimodal size distribution

(b) Truncated Gaussian size distribution

FIG. 5. (Color online) Extinction spectra of monodisperse and polydisperse aggregates of type 2. Results are shown for an aggregate consisting of $N = 50$ particles. The interparticle gap for all nearest-neighbor pairs is $h = 0.2$ nm (black solid line), 0.3 nm (blue dashed line), and 0.5 nm (red dot-dashed line).

Gaussian distribution, the particle sizes are more likely to be close to the average value and the effect of polydispersity is weaker. Similarly to the case of a dimer and a trimer, but in contrast to the results of Refs. 22 and 23, the amplitude of the long-wavelength tail tends to increase with the degree of polydispersity.

In addition to the coupled-multipole calculations, we report in Fig. 4 the spectra computed in the DA with and without the phenomenological geometrical rescaling. The data reveal a considerable inaccuracy of the DA. Despite the apparent similarity of the long-wavelength tails obtained by both approaches, the spectral region near the Fröhlich resonance is not captured properly by the DA.

2. *Aggregates of type 2*

This type of aggregate allows one to study the effect of particle radii polydispersity in its "pure form" since polydispersity of the interparticle gaps is, in this case, suppressed. Extinction spectra computed by the coupled-multipole method are shown in Fig. 5. We note that a significant broadening of the long-wavelength tail is observed in the spectra of bimodal aggregates when the degree of polydispersity is increased. This result is unexpected and a similar tendency was not observed in the DA-based simulations of Refs. 22–24.

On the other hand, the spectra of truncated Gaussian aggregates depend on the degree of polydispersity quite insignificantly.

3. *Aggregates of type 3*

This type of polydisperse aggregate is the most realistic. The equilibrium gap widths in this type of aggregate depend on all relevant physical parameters and vary from 0.1 nm (between the largest particles) to 0.3 nm (between the smallest particles), with the average value of $\langle h \rangle = 0.2$ nm. The optical spectra are shown in Fig. 6. In the case of bimodal aggregates, a significant broadening of the long-wavelength spectral tail is obtained when the degree of particle polydispersity is

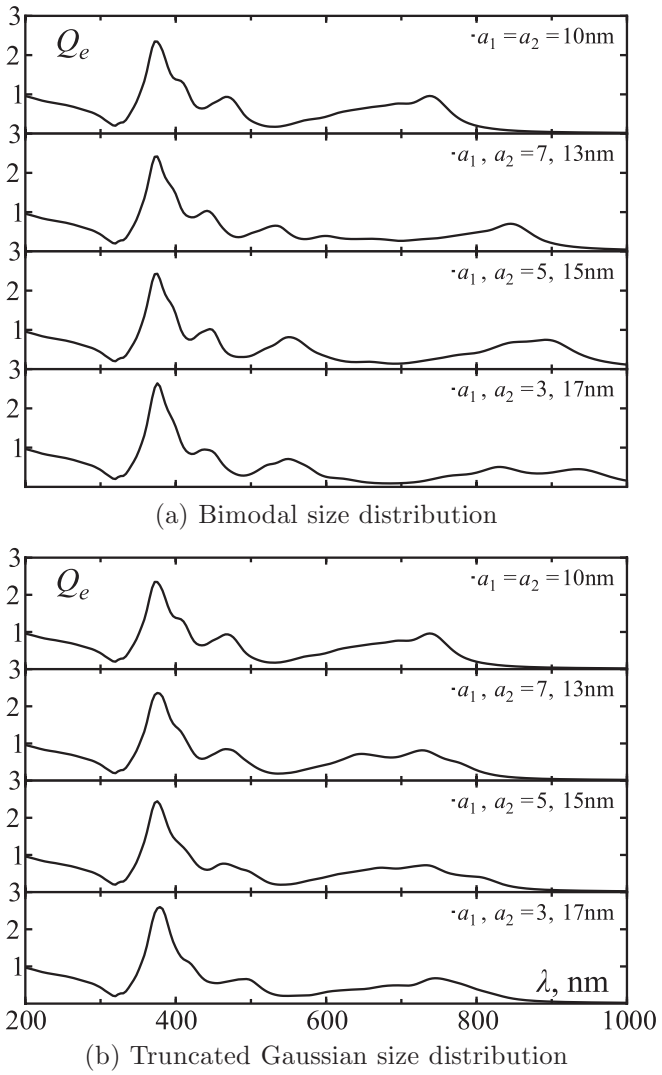

(a) Bimodal size distribution

(b) Truncated Gaussian size distribution

FIG. 6. Extinction spectra of aggregates of type 3. Results are shown for an aggregate consisting of $N = 50$ particles. In the bimodal case, the interparticle gap depends on the sizes of nearest-neighbor particles as follows: $h = 0.1$ nm for a pair of two particles of the larger radius, $h = 0.2$ nm for a pair of two particles of different radii, and $h = 0.3$ nm for a pair of particles of the smaller radius. In the Gaussian case, the gaps were computed self-consistently from the condition of mechanical equilibrium.

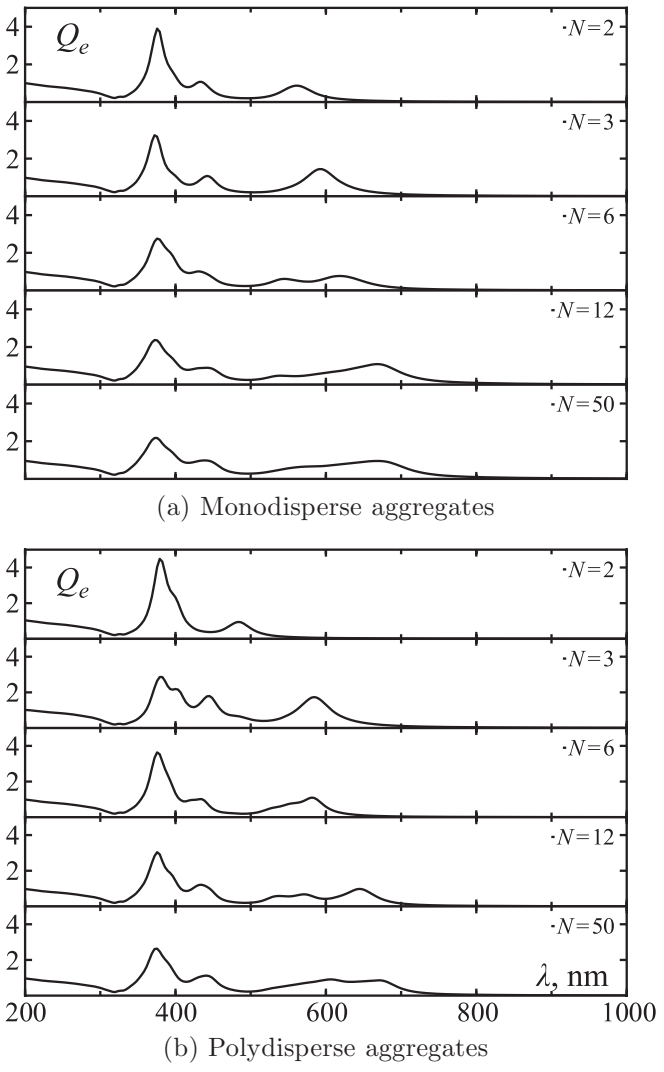

(a) Monodisperse aggregates

(b) Polydisperse aggregates

FIG. 7. Extinction spectra of monodisperse ($a_1 = a_2 = 10$ nm) and truncated Gaussian polydisperse ($a_1 = 3$ nm, $a_2 = 17$ nm) aggregates of type 1 with different numbers of particles N, as labeled. Computed by the coupled-multipole method with $L = 40$. In all case, $\langle h \rangle = 0.3$ nm.

increased. However, in truncated Gaussian aggregates, this tendency is weakened. Overall, we find that the introduction of particle polydispersity in type-3 aggregates does not suppress the computed long-wavelength spectral wing. This finding is, again, in contrast to the results of previous studies.[22–24]

D. Dependence of the spectra on the number of particles in an aggregate

It is often of interest to study the extinction spectra of polydisperse hydrosols at different stages of the aggregation process. It is clear that the spectra of isolated particles are quite different from those of dimers, the latter are different from those of trimers, etc. At some moderate values of N, a limit is usually reached and no further dependence of spectra on N is observed. However, when N is further increased, the quasistatic approximation may become inaccurate and qualitatively new effects can emerge. In this section, we study the dependence of the spectra on the number of particles in an aggregate.

We start with relatively small aggregates within the quasistatic limit. In Fig. 7, we plot the spectra of monodisperse and polydisperse aggregates of type 1 with different numbers of particles per aggregate, N. The average interparticle gap in these aggregates is $\langle h \rangle = 0.3$ nm and the spectra are computed by the coupled-multipole method with $L = 40$. One tendency that can be seen from comparing Figs. 7(a) and 7(b) is that the effects of polydispersity are suppressed when N is increased.

In Fig. 8 we also show the spectra obtained within the DA but beyond the quasistatics and for much larger values of N (up to $N = 10^3$). The DA is expected to be inaccurate for the interparticle gaps considered here. However, the inaccuracy is more pronounced near the Fröhlich frequency where the extinction is too small. The long-wavelength spectral tail is

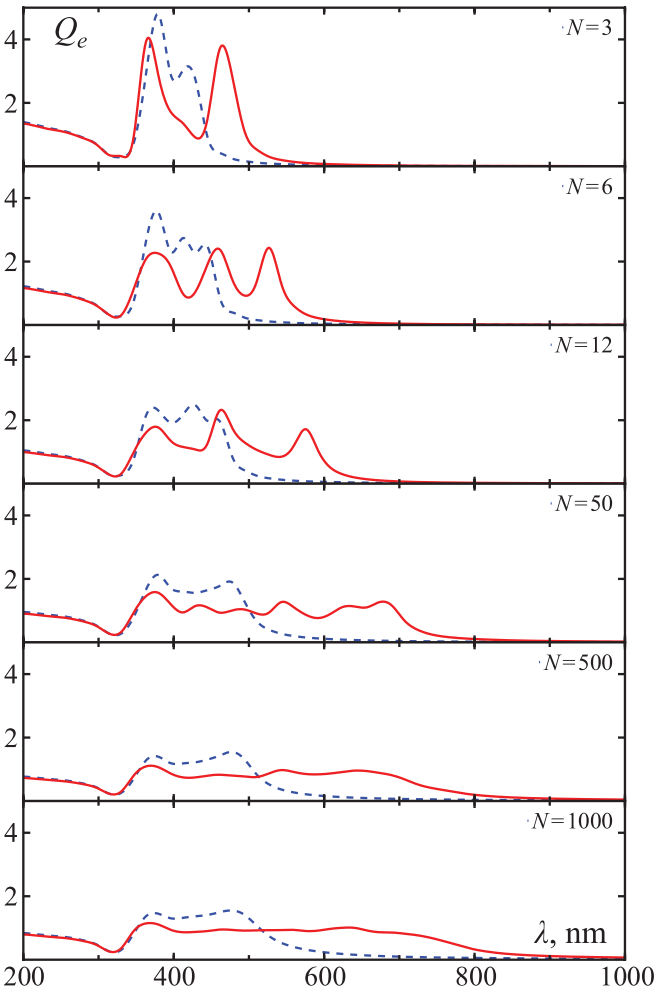

FIG. 8. (Color online) Spectra of truncated Gaussian aggregates of type 1 with the same a_1 and a_2 as in Fig. 7, but with much larger values of N, computed within the DA and beyond the quasistatic approximation, with and without the phenomenological rescaling. The rescaling parameter is $\xi = 1$ (blue dashed line) and 1.4 (red solid line).

qualitatively reproduced by selecting the geometrical rescaling parameter $\xi = 1.4$. The data of Fig. 8 indicate that, when N is increased, the long-wavelength spectral wing is extended further toward the infrared and becomes smoother. A similar tendency was observed in the coupled-multipole simulations, although the latter could not be carried out for N much larger than 50 due to the computational constraints.

Finally, in Fig. 9, we plot the extinction spectra, averaged over three polarizations, of bimodal aggregates with the number of particles $N = 3$ and 50. The orientation of particles in aggregates with $N = 3$ is arbitrary, in contrast to the linear trimer, whose spectra are calculated only for the longitudinal polarization (see Fig. 2). It was found that the extent of the spectral tail for the case of a three-particle aggregate does not significantly depend on the particles' different arrangements [the possible arrangements are (a_1,a_2,a_1); (a_1,a_1,a_2); (a_2,a_1,a_2), and (a_1,a_2,a_2)]. In the case of the first three arrangements, the extent of the spectral wing is noticeably decreased when the degree of polydispersity is increased. In the case of the fourth arrangement (a_1,a_2,a_2), this effect is

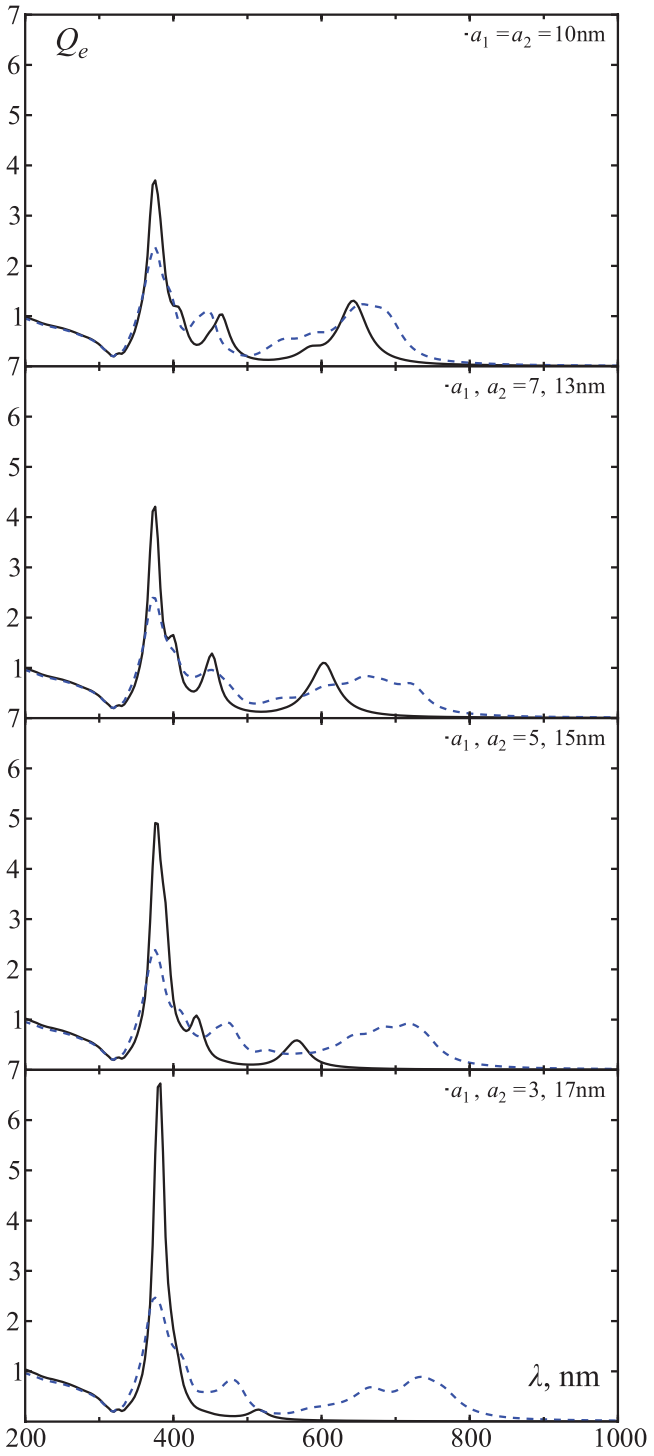

FIG. 9. (Color online) Extinction spectra of bimodal aggregates of type 2 with different numbers of particles: $N = 3$ (solid black line) and 50 (blue dashed line). Interparticle gap is $h = 0.2$ nm, and the degree of polydispersity is as labeled. Computed by the coupled-multipole method with $L = 40$.

less pronounced (a_1 and a_2 are the radii of the smaller and larger particles, respectively). Here we observe a somewhat unusual tendency. For small N, an increase in the degree of particle polydispersity results in a suppressed long-wavelength spectral wing, while for $N = 50$, it is noticeably broadened. For $6 \leqslant N \leqslant 12$, the wing appears not be affected. This

observation can be explained by the fact that, in multiparticle aggregates, there is a nonzero probability to find several particles of maximum sizes located in a close vicinity of each other and forming a "resonant domain." The spectra of these domains have stronger long-wave shifts than the spectra of trimers of the (a_1,a_2,a_1), (a_1,a_1,a_2), and (a_2,a_1,a_2) types. For example, the maximum extent of the spectral wing for a trimer of the type (17 nm,13 nm,17 nm) is 725 nm, whereas for a trimer of the type (17 nm,3 nm,17 nm), the spectral wing extends to 620 nm.

IV. CONCLUSIONS

We have computed the optical spectra of naturally occurring off-lattice aggregates of spherical silver nanoparticles, taking into account the interparticle polymer layers (adlayers) and the size polydispersity of the metal cores. We have used both the coupled-multipole method with the maximum multipole order $L = 40$ and the dipole approximation with and without phenomenological rescaling.[26] Previous studies of the effects of polydispersity[22–24] have been limited to the DA and did not account for the presence of adlayers. It was found in Refs. 22–24 that polydispersity of the metal cores tends to suppress the long-wavelength spectral tail in the extinction spectra. We have found, however, that with the proper account of adlayers and multipolar interaction, this is not necessarily so. In fact, in realistic geometries, the polydispersity tends to enhance the long-wavelength spectral tail.

Therefore, special attention should be paid to quantification of the adlayers (interparticle gaps), whose magnitude can modify quite radically the effect of polydispersity on the spectra. Under conditions similar to those employed in Refs. 22–24 (aggregates of type 1), we obtained a qualitatively similar effect, that is, suppression of the long-wavelength spectral tail by the polydispersity. However, in more realistic aggregates of types 2 and 3, this effect is either absent or reversed. We thus conclude that use of polydisperse aggregates of type 1 in optical calculations may lead to incorrect results. Perhaps the most practically important conclusion of this paper is that preparation of strictly monodisperse nanocolloids is not required. The experimentally observed plasmonic absorption band is not suppressed by particle polydispersity in realistic systems.

On the other hand, we must acknowledge that the spectra computed in this paper do not extend as far into the infrared as do the experimental spectra.[1,3,7,14,38] This indicates that the electromagnetic model employed here and in many other similar works is deficient. But this deficiency is not easy to pinpoint. It appears that it is not related to excitation of high multipole orders, or to particle polydispersity, or to the existence of adlayers and interparticle gaps. Further development of the theory will require taking into account nonsphericity and the crystallographic axes of the nanoparticles, a more accurate electromagnetic description of the adlayers, inclusion of the nonlocal electromagnetic response of the metal, and an accurate account of quantum finite-size effects. In addition, generalization of the coupled-multipole method beyond the quasistatic approximation is expected to provide more smooth and realistic spectra, especially for large aggregates, similarly to what we have observed within the DA. We emphasize that, theoretically, such a generalization is well known.[39–41] However, its practical implementation in the context of large metallic nanoaggregates is impeded by high computational costs.

ACKNOWLEDGMENTS

This work was supported by grants from the following foundations of the Russian Federation: Presidium of RAS, OFN RAS, and SB RAS.

[1] U. Kreibig and M. Vollmer, *Optical Properties of Metal Clusters* (Springer-Verlag, Berlin, 1995).
[2] V. M. Shalaev, *Nonlinear Optics of Random Media: Fractal Composites and Metal Dielectric Films* (Springer-Verlag, Berlin, 2000).
[3] S. V. Karpov and V. V. Slabko, *Optical and Photophysical Properties of Fractal-Structured Metal Sols* (Russian Academy of Sciences, Siberian Branch, Novosibirsk, 2003).
[4] V. V. Klimov, *Nanoplasmonics* (Fizmatlit, Moscow, 2009).
[5] V. I. Roldugin, Russ. Chem. Rev. **72**, 913 (2003).
[6] M. A. Noginov *et al.*, Opt. Lett. **31**, 3022 (2006).
[7] M. Quinten, *Optical Properties of Nanoparticle Systems: Mie and Beyond* (Wiley-VCH, Weinheim, Germany, 2011).
[8] S. V. Karpov *et al.*, JETP Lett. **48**, 571 (1988).
[9] Y. E. Danilova, A. I. Plekhanov, and V. P. Safonov, Physica A **185**, 61 (1992).
[10] V. P. Safonov, V. M. Shalaev, V. A. Markel, Y. E. Danilova, N. N. Lepeshkin, W. Kim, S. G. Rautian, and R. L. Armstrong, Phys. Rev. Lett. **80**, 1102 (1998).
[11] S. V. Karpov, A. K. Popov, and V. V. Slabko, Tech. Phys. **73**, 90 (2003).
[12] A. V. Butenko *et al.*, Z. Phys. D **17**, 283 (1990).
[13] Y. E. Danilova, S. G. Rautian, and V. P. Safonov, Bull. Russ. Acad. Sci. Phys. **60**, 374 (1996).
[14] Y. E. Danilova, N. N. Lepeshkin, S. G. Rautian, and V. P. Safonov, Physica A **241**, 231 (1997).
[15] N. N. Lepeshkin *et al.*, J. Nonlinear Opt. Phys. Mater. **8**, 191 (1999).
[16] S. V. Karpov, M. K. Kodirov, A. I. Ryasiyanskiy, and V. V. Slabko, Quantum Electron. **31**, 904 (2001).
[17] R. A. Ganeev, A. I. Ryasnyansky, S. R. Kamalov, and T. B. Usmanov, Physica D **34**, 1602 (2001).
[18] V. P. Drachev *et al.*, Sov. Phys. JETP **95**, 901 (2002).
[19] A. P. Gavrilyuk and S. V. Karpov, Appl. Phys. B **97**, 163 (2009).
[20] A. P. Gavrilyuk and S. V. Karpov, Appl. Phys. B **102**, 65 (2011).
[21] N. G. Khlebtsov and A. G. Melnikov, J. Colloid Interface Sci. **163**, 145 (1994).
[22] S. V. Perminov, S. G. Rautian, and V. P. Safonov, Opt. Spectrosc. **95**, 616 (2003).
[23] S. V. Perminov, S. G. Rautian, and V. P. Safonov, Sov. Phys. JETP **98**, 691 (2004).
[24] Z. Naeimi and M. F. Miri, Phys. Rev. B **80**, 224202 (2009).
[25] *Adsorption from Solution at the Solid/Liquid Interface*, edited by G. Parfitt and C. Rochester (Academic Press, London, 1983).

[26]V. A. Markel and V. M. Shalaev, J. Opt. Soc. Am. A **18**, 1112 (2001).
[27]J. E. Sansonetti and J. K. Furdyna, Phys. Rev. B **22**, 2866 (1980).
[28]P. B. Johnson and R. W. Christy, Phys. Rev. B **6**, 4370 (1972).
[29]F. Hache, D. Ricard, and C. Flytzanis, J. Opt. Soc. Am. B **3**, 1647 (1986).
[30]S. G. Rautian, Sov. Phys. JETP **85**, 451 (1997).
[31]V. A. Markel, V. M. Shalaev, E. B. Stechel, W. Kim, and R. L. Armstrong, Phys. Rev. B **53**, 2425 (1996).
[32]D. W. Macowski, Appl. Opt. **34**, 3535 (1995).
[33]V. A. Markel, V. N. Pustovit, S. V. Karpov, A. V. Obuschenko, V. S. Gerasimov, and I. L. Isaev, Phys. Rev. B **70**, 054202 (2004).
[34]E. M. Purcell, Astrophys. J. **158**, 433 (1969).
[35]B. T. Draine, Astrophys. J. **333**, 848 (1988).
[36]V. A. Markel, J. Opt. Soc. Am. B **12**, 1783 (1995).
[37]S. V. Karpov *et al.*, Colloid J. **71**, 313 (2009).
[38]S. M. Heard, F. Griezer, C. G. Barrachough, and J. V. Sandera, J. Colloid Interface Sci. **93**, 545 (1983).
[39]D. W. Mackowski and M. Mishchenko, J. Opt. Soc. Am. A **13**, 2266 (1996).
[40]K. A. Fuller and D. W. Mackowski, in *Light Scattering by Nonspherical Particles*, edited by M. I. Mishchenko, J. W. Hovenier, and L. D. Travis (Academic Press, New York, 2000), Chap. 8, pp. 226–273.
[41]Y. L. Xu and B. A. S. Gustafson, J. Quant. Spectrosc. Radiat. Transfer **70**, 395 (2001).